JCB
THE JOURNAL OF CELL BIOLOGY
VOL. 210, NO. 7, SEPTEMBER 28, 2015

Src Limits Stem Cell Differentiation

Mitochondria Direct Neutrophil Chemotaxis

Alternative Splicing Saves Glycolytic Cancer Cells

Glia Spring to the Retina's Defense

www.jcb.org

Published September 28, 2015

Müller glia provide essential tensile strength to the developing retina

Ryan B. MacDonald,[1] Owen Randlett,[1] Julia Oswald,[1] Takeshi Yoshimatsu,[2] Kristian Franze,[1] and William A. Harris[1]

[1]Department of Physiology, Development and Neuroscience, University of Cambridge, Cambridge CB2 3DY, England, UK
[2]Department of Biological Structure, University of Washington, Seattle, WA 98195

To investigate the cellular basis of tissue integrity in a vertebrate central nervous system (CNS) tissue, we eliminated Müller glial cells (MG) from the zebrafish retina. For well over a century, glial cells have been ascribed a mechanical role in the support of neural tissues, yet this idea has not been specifically tested in vivo. We report here that retinas devoid of MG rip apart, a defect known as retinoschisis. Using atomic force microscopy, we show that retinas without MG have decreased resistance to tensile stress and are softer than controls. Laser ablation of MG processes showed that these cells are under tension in the tissue. Thus, we propose that MG act like springs that hold the neural retina together, finally confirming an active mechanical role of glial cells in the CNS.

Introduction

The nervous system is one of the softest tissues in the body (Franze et al., 2013; Swift et al., 2013), with a consistency similar to that of cream cheese. Yet it is also the most highly organized tissue in the body, composed of neurons and glial cells arranged into discrete layers. How this incredibly soft and complex tissue maintains its integrity throughout life, despite the many physical stresses imparted on it, remains a mystery. The retina, an outpocket of the central nervous system, is constantly exposed to physical stresses (Franze et al., 2011), which can lead to a tearing of the retinal tissue along the layers known as retinoschisis. The neurons of the retina do not appear to provide much structural support to the tissue, as various genetic manipulations have shown that any of the neuronal types can been completely eliminated from the tissue, either singly (Tomita et al., 2000; Kay et al., 2001; Green et al., 2003; Randlett et al., 2013) or in various combinations (Randlett et al., 2013), without reported structural consequences.

More than 150 years ago, Rudolf Virchow first described glial cells, which he likened to "Nervenkitt" or nerve-putty. Expecting them to provide mechanical support to neurons, he termed them "neuroglia" (after the Greek word for glue; Virchow, 1856). While glial cells are now appreciated for their many roles in neural development and function (Allen and Barres, 2009; Reichenbach and Bringmann, 2013; Kettenmann and Ransom, 2013), Virchow's earliest speculation of their involvement in physical support persists in most modern textbooks of basic neuroscience, despite a lack of direct experimental proof. There is some evidence both for and against Virchow's idea. First, investigations into the biomechanical properties of glial cells revealed that they are twice as soft as their neighboring neurons, indicating that glia cannot provide a rigid structural framework that neurons can cling to (Lu et al., 2006). However, other studies showed that glial cells in the retina are responsive to mechanical signals (Lindqvist et al., 2010) and quickly recover their shape after deformation (Lu et al., 2006), suggesting that they might be able at least to withstand tensile stresses. Additionally, the elimination of myelin and oligodendrocytes deceases the tensile strength and stiffness of the spinal cord exposed to large deformations ex vivo (Shreiber et al., 2009). However, whether glial cells are mechanically important to neural tissue in vivo if it is exposed to physiologically relevant strains is currently unknown. To investigate the cellular mechanism of neural tissue integrity, it is therefore critical to remove the glial cells from the tissue, while leaving the neurons intact. Here, we eliminated Müller glia cells (MG) specifically from the zebrafish retina by manipulating Notch signaling at a critical time point for gliogenesis. Retinal tissue lacking glial cells was less capable of resisting stretch and had a strong tendency to rip apart. We provide evidence that MG act like taut springs that hold the neural tissue of the retina together.

Results and discussion

Zebrafish MG are generated by 48 h postfertilization (hpf)

The zebrafish retina, like all vertebrate retinas, consists of five major neuronal and one glial type, MG (Cajal, 1972). MG are

Correspondence to Kristian Franze: kf324@cam.ac.uk; or William A. Harris: wah20@cam.ac.uk

Abbreviations used in this paper: AFM, atomic force microscopy; Cralbp, cis-retinaldehyde binding protein; DAPT, *N*-[*N*-(3,5-difluorophenacetyl)-L-alanyl]-*S*-phenylglycine t-butyl; dpf, days postfertilization; GCL, ganglion cell layer; hpf, hours postfertilization; INL, inner nuclear layer; MG, Müller glia cells; RPC, retinal progenitor cell.

Supplemental Material can be found at:
http://jcb.rupress.org/content/suppl/2015/09/25/jcb.201503115.DC1.html
Original image data can be found at:
http://jcb-dataviewer.rupress.org/jcb/browse/10552

The Rockefeller University Press $30.00
J. Cell Biol. Vol. 210 No. 7 1075–1083
www.jcb.org/cgi/doi/10.1083/jcb.201503115

Published September 28, 2015

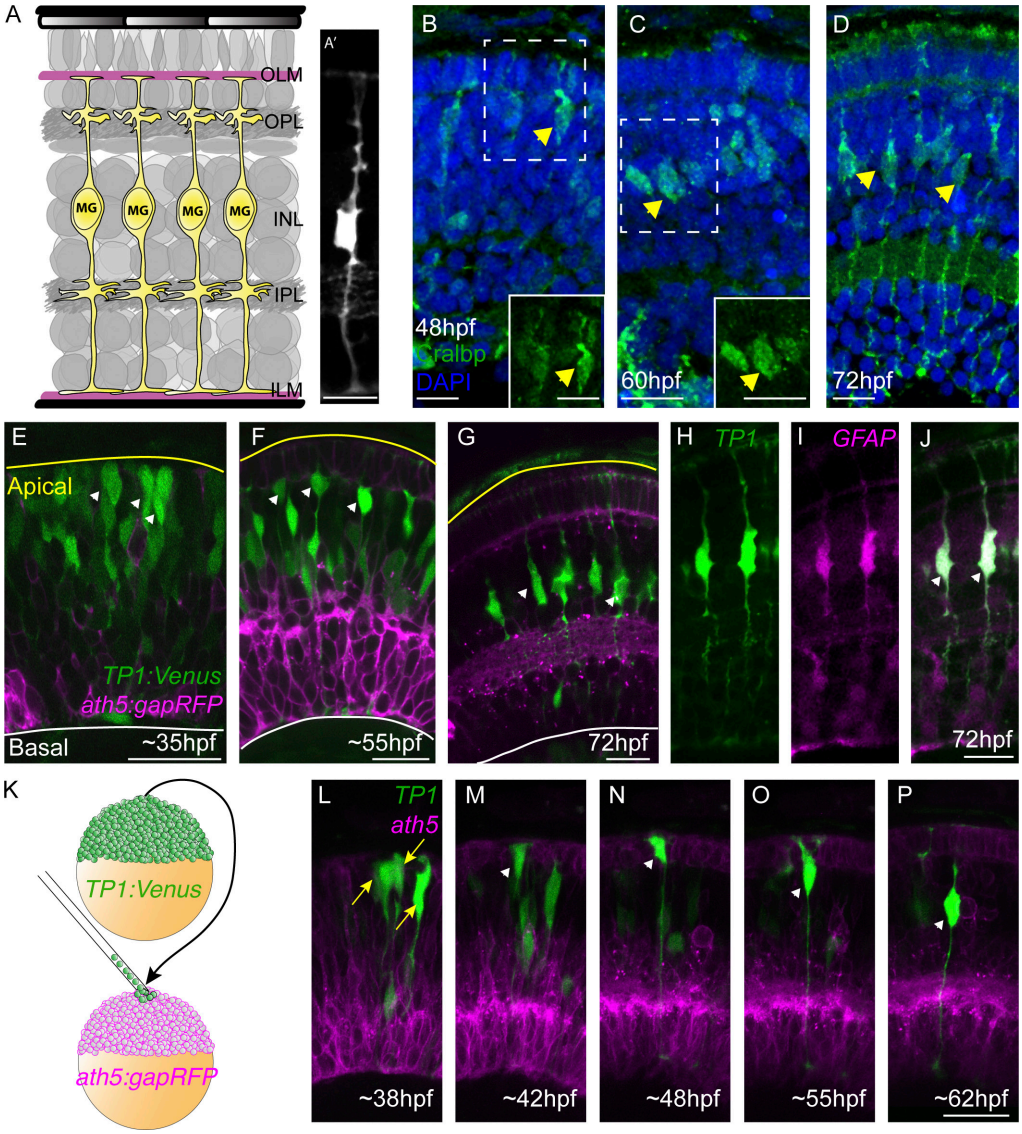

Figure 1. **Notch signaling is active in the nascent and mature MG in the developing retina.** (A and A′) MG span the entirety of the three neural layers from the inner limiting membrane (ILM) to the outer nuclear layer (OLM). (B) Using Cralbp as an early marker for MG specification in cryosections, we see expression on the apical side of the retina at 48 hpf. (C and D) This expression increases in the INL by 60 hpf (C), and was strongly expressed at 72 hpf in mature MG (D). (E) In whole-mount samples at 35 hpf, many cells within the nascent retina have Notch activity (green), especially on the apical side of the retina (arrowheads). (F) Notch activity at 55 hpf appears in radial cells on the apical side of the retina (arrowheads). (G) Notch activity is restricted to MG at 72 hpf. (H–J) The Notch-positive cells in the mature retina are MG, as shown by the overlap in the *TP1:Venus* and *GFAP:dTomato* transgenic constructs (arrows). (K) The transplantation strategy to generate clones of *TP1:Venus* (green) embryos into the *ath5:gapRFP* host (magenta). (L–P) Panels from a time-lapse movie of a clone in a living zebrafish retina ($n = 6$). (L) Notch is active in multiple cells in the clone at 38 hpf. Notch activity is progressively restricted until a single cell maintains Notch on the apical side of the retina at 42 hpf (M). Notch activity increases in this cell at 48 hpf (N), and at 55 hpf (O) it migrates basally and will position itself within the INL and begin to mature by 62 hpf (P). Figures always show the apical side of the retina at the top and basal at the bottom. OPL, outer plexiform layer; IPL, inner plexiform layer. Bars, 10 µm.

the only cells to span the width of the mature tissue from the inner to the outer limiting membranes (Fig. 1 A). During retinogenesis, postmitotic cells are generated from retinal progenitor cells (RPCs) in a conserved histogenetic order, in which MG are among the last cells to be generated (Rapaport et al., 2004). To identify when MG first appear in the zebrafish retina, we tested several MG markers. Of these, an antibody against cis-retinaldehyde binding protein (Cralbp) proved to be the earliest marker for MG, showing expression on the apical side of the retina as early as 48 hpf (Fig. 1 B). MG cell bodies, labeled for Cralbp, first appeared in the inner nuclear layer (INL) at ~60 hpf (Fig. 1 C) and obtained their mature morphology by 72 hpf (Fig. 1 D).

Notch signaling is critical for the specification of MG in several species (Dorsky et al., 1995; Furukawa et al., 2000; Bernardos et al., 2005). To assess whether this might be the case in fish, we first examined the dynamics of Notch signaling in retinal cells using the transgenic reporter line *Tg(TP1:Venus-PEST)* (Ninov et al., 2012). This transgene consists of the Notch responsive element (TP1), which controls the expression of the destabilized fluorescent protein, Venus-PEST (Aulehla et al., 2008; Parsons et al., 2009). Thus, we could rapidly visualize the changes in Notch activity over time. Notch was active in many cells within the developing retina at 35 hph (Fig. 1 E). However, it became progressively restricted, and by 72 hpf Notch activity

Published September 28, 2015

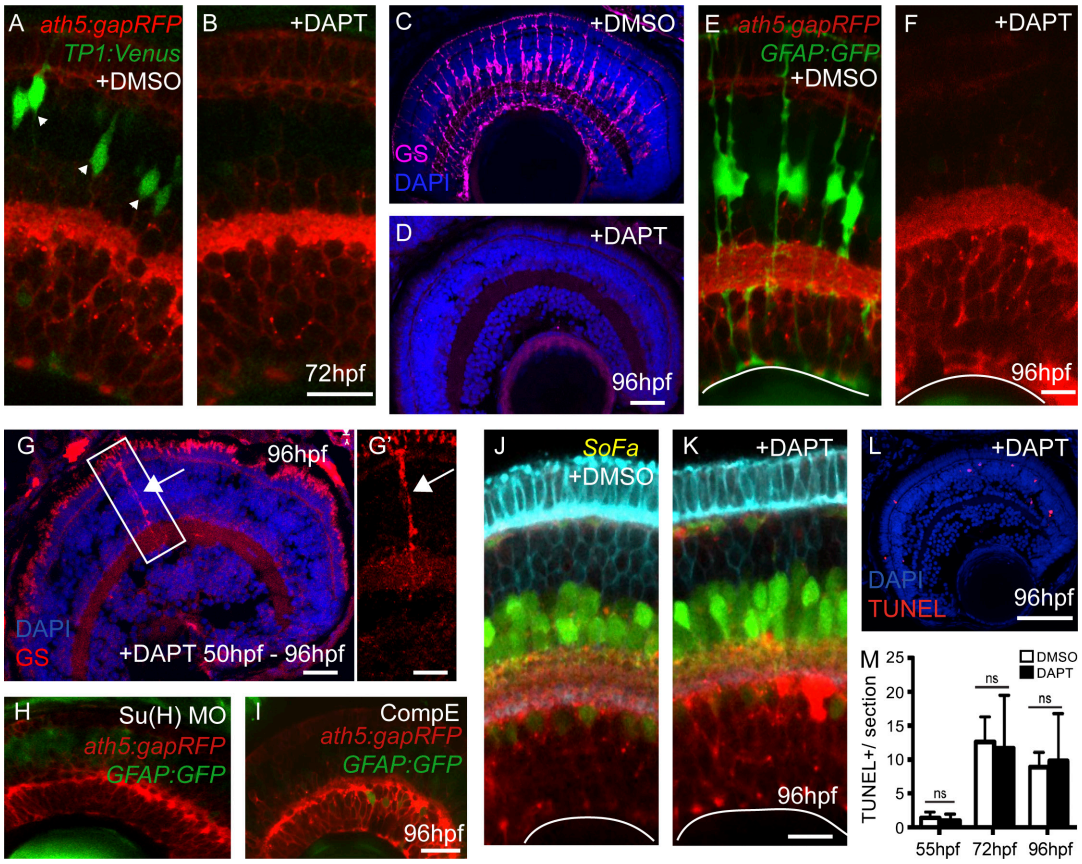

Figure 2. **Blocking Notch activity during retinogenesis results in a loss of MG.** (A and B) Treatment with DAPT at 45 hpf results in the loss of Notch activity (green) in whole-mount retinas at 72 hpf. (C and D) In cryosections, MG specifically express glutamine synthetase (GS), but after DAPT treatment the retina is completely lacking in GS expression. (E and F) DAPT treatment of double transgenic fish, *ath5:gapRFP;GFAP:GFP*, results in a complete loss of GFP-expressing MG in the retina of the transgenic line *GFAP:GFP*. (G) Treatment with DAPT at 50 hpf is too late to completely block MG specification in the central retina (arrow). G′ shows the boxed region. (H and I) There are reduced *GFAP:GFP*-positive cells in the central retina after Su(H) morpholino injection or treatment with Compound E, another γ-secretase inhibitor, at 96 hpf, similar to DAPT treatments. (J and K) Retinal neurons are specified and patterned properly in the *SoFa* fish. (L and M) There is no increase in cell death (TUNEL+ cells) in the absence of MG (mean + SEM, *n* = 10 retinas). Bars: (A–D) 25 µm; (E–G) 20 µm; (G′) 10 µm; (H and I) 30 µm; (J and K) 20 µm; (L) 50 µm.

was present only in MG (Fig. 1, F–J). To see this progressive restriction at the level of a single clone, we transplanted individual blastomeres from *Tg(TP1:VenusPEST)* into *Tg(ath5:gapRFP)* embryos, where most retinal neurons are labeled with membrane RFP (Zolessi et al., 2006; Fig. 1 K). At ∼38 hpf, we saw many Notch-positive clusters of cells, representing individual clones in the host retina (Fig. 1 L and Video 1). As development progressed, however, most of these cells lost Notch activity, and by 48 hpf, we often found that only one cell within a clone retained strong Notch activity on the apical side of the retina (Fig. 1, M and N, arrowheads). At ∼55 hpf, Notch-positive cells migrated basally into the INL (Fig. 1 O), and by 62 hpf obtained an MG-like morphology (Fig. 1 P).

Specific elimination of MG from the developing retina

The data above suggest that MG arise at ∼48 hpf, which is after most other cell types in the zebrafish retina are generated (Hu and Easter, 1999; He et al., 2012). Therefore, to specifically block the formation of MG, we added the γ-secretase inhibitor *N*-[*N*-(3,5-difluorophenacetyl)-L-alanyl]-*S*-phenylglycine t-butyl (DAPT) to the embryo media just before this stage at ∼45 hpf. This treatment resulted in reduced Notch levels (Fig. 2, A and B). In such treated fish, there was no staining for MG-specific markers (Fig. 2, C and D; and Fig. S1; Randlett et al., 2013) or transgenes (Fig. 2, E and F) in the retina until at least 120 hpf. Exposing fish to DAPT even a few hours later (at ∼50 hpf) was too late to prevent MG specification in the central retina (Fig. 2, G and G′). We also manipulated the Notch pathway with a second γ-secretase inhibitor, Compound E, and by knocking down the Notch effector Su(H), using a translation blocking morpholino (Sieger et al., 2003). Consistent with DAPT treatments, these developing retinas also lacked MG (Fig. 2, H and I).

We found it surprising that embryonic retinas lacking MG due to DAPT treatment at 45 hpf showed an apparently normal cellular architecture of all the neuronal cell types in the retina, as clearly demonstrated in the Spectrum-of-fates zebrafish line (Fig. 2, J and K; Almeida et al., 2014). Retinas of treated embryos did not display any significant changes in cell death from 48 hpf to 120 hpf (Fig. 2, L and M). This was surprising because MG have many physiological functions in the retina (Bringmann et al., 2006; Reichenbach and Bringmann, 2013). Previous work has also shown that, when MG in the adult mouse retina are ablated by cell-specific killing, there are defects in retinal vascularization, structure, and function, including the wide-scale disorganization and apoptosis of photoreceptor cells (Shen et al., 2012; Byrne et al., 2013). In contrast, we saw only very modest effects on photoreceptor structure and

Published September 28, 2015

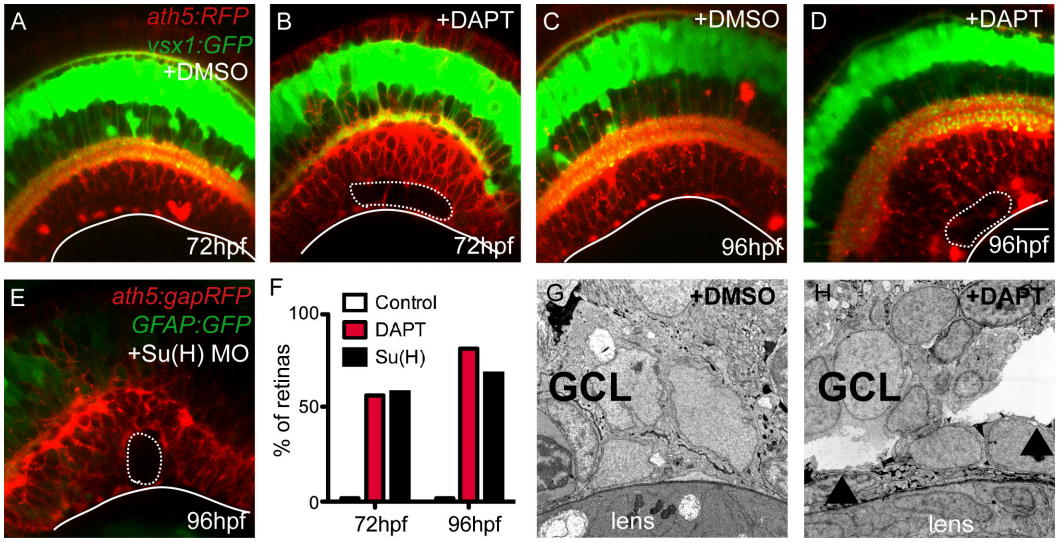

Figure 3. **Retinas lacking MG show intraretinal tears or "retinoschisis" in the GCL.** Confocal images of the living fish retina in vivo. The retina is double transgenic for both *vsx1:GFP*, labeling most bipolar cells (green), and *ath5:gapRFP*, strongly labeling retinal ganglion cells in the GCL (red). (A–D) At 72 hpf (A and B) and 96 hpf (C and D), DAPT-treated retinas lacking MG have a specific ripping in the GCL (dashed line) along the basal surface of the retina (white solid line). (E) The *Su(H)* morphant retina does not have MG, as shown by the loss of *GFAP:GFP*-positive cells. (F) We did not observe any ripping within the retina of control fish. However, ripping in the GCL occurs in similar proportions in *Su(H)* morphant and DAPT-treated retinas ($n = 50$ retinas for each condition). (G and H) Electron microscopy shows local ripping within the GCL along the basal-most portion of the retina (arrowheads). Bars, 20 µm.

no significant change in neural survival in our study on the embryonic zebrafish retina. However, at early embryonic stages, vision is just beginning (Easter and Nicola, 1996), and it is likely that the role of MG in promoting photoreceptor survival becomes more crucial after photoreceptors become fully functional later in development.

The loss of MG results in retinoschisis

Strikingly, retinas lacking MG frequently showed a splitting of the neural retina, or retinoschisis, specifically in the ganglion cell layer (GCL) between ganglion cell bodies (Fig. 3; Fig. S2, A–D; and Videos 2 and 3). This retinoschisis varied in severity within the GCL between embryos (Fig. S2, A–D). There were occasional pigment granules within the neural layers and disorganization of the photoreceptor layer, but these defects were less penetrant than the ripping phenotype and did not correlate strongly with the retinoschisis, suggesting that these may be minor independent effects of interfering with Notch signaling (Fig. S3).

To determine when these rips first appeared, we examined MG-less retinas at a variety of stages. We did not find any evidence for ripping at 33 hpf and 48 hpf (Fig. S2, E–G); however, by 96 hpf, 50% of treated retinas exhibited retinoschisis (Fig. 3, A–D and F). The ripping was not a nonspecific effect of the pharmacological inhibitor, as we saw similar retinoschisis phenotypes in Su(H) morphants (Fig. 3, E and F) and Compound E–treated retinas (not depicted). Additionally, when exposure to DAPT treatment started at 72 hpf rather than at 45 hpf, MG started to develop in the central retina, and there was no retinoschisis even 2 d later (Fig. S2 H). As the knockdown of her4, which is a downstream Notch target specifically expressed only in MG and bipolar cells (Fig. S2 I), also resulted in a reduction of MG in the retina and a concomitant retinoschisis phenotype (~10% affected; Fig. S2 J) without interfering with Notch signaling in other neurons, it is likely that the observed phenotype is a direct consequence of the loss of MG rather than Notch signaling. While we cannot exclude the possibility that bipolar cells provide some physical support to the retina, this is unlikely, as their development appears unperturbed in the DAPT treatment or her4 knockdown, and their basal processes do not extend into the GCL where the ripping occurs.

The retinoschisis phenotype observed in our study is reminiscent of degenerative retinoschisis, a human condition characterized by the splitting of the retina into two layers (Samuels and Fuchs, 1952; Straatsma and Foss, 1973). A hereditary X-linked form of retinoschisis is characterized by intraretinal splitting, which is attributed to mutations in the *Retinoschisin* gene (Sauer et al., 1997). MG transport the secreted Retinoschisin protein to the inner retina (Reid and Farber, 2005), but MG-specific misexpression of Retinoschisin is not sufficient to rescue a mouse model of the disease (Byrne et al., 2014). However, the involvement of MG in this disease remains a matter of debate (Molday et al., 2012). In the zebrafish retina lacking MG, Retinoschisin protein expression appears to be normal (Fig. S2, K and L), indicating that the observed phenotype is likely more similar to the degenerative form of retinoschisis and not the genetic form of the disease.

MG act like taut springs, providing resilience and stiffness to the retina

To test whether MG provide mechanical resilience to the retina, we applied controlled tensile forces (i.e., stretch) to retinas with and without MG, and measured their resulting deformations using atomic force microscopy (AFM; Fig. 4 A; Franze, 2011). At 33 hpf and 48 hpf, when radially oriented RPCs are still present in the retina, treated and control retinas showed no difference in tissue deformation (Fig. 4 B). However, at 72 hpf, we found a significantly larger increase in tissue deformation, and thus a decrease in resistance to tensile forces, in retinas without MG (Fig. 4 C). Interestingly, control retinas did not deform significantly more at 72 hpf than they do at 33 hpf, suggesting that at early stages it is the radially oriented RPCs that are providing

Published September 28, 2015

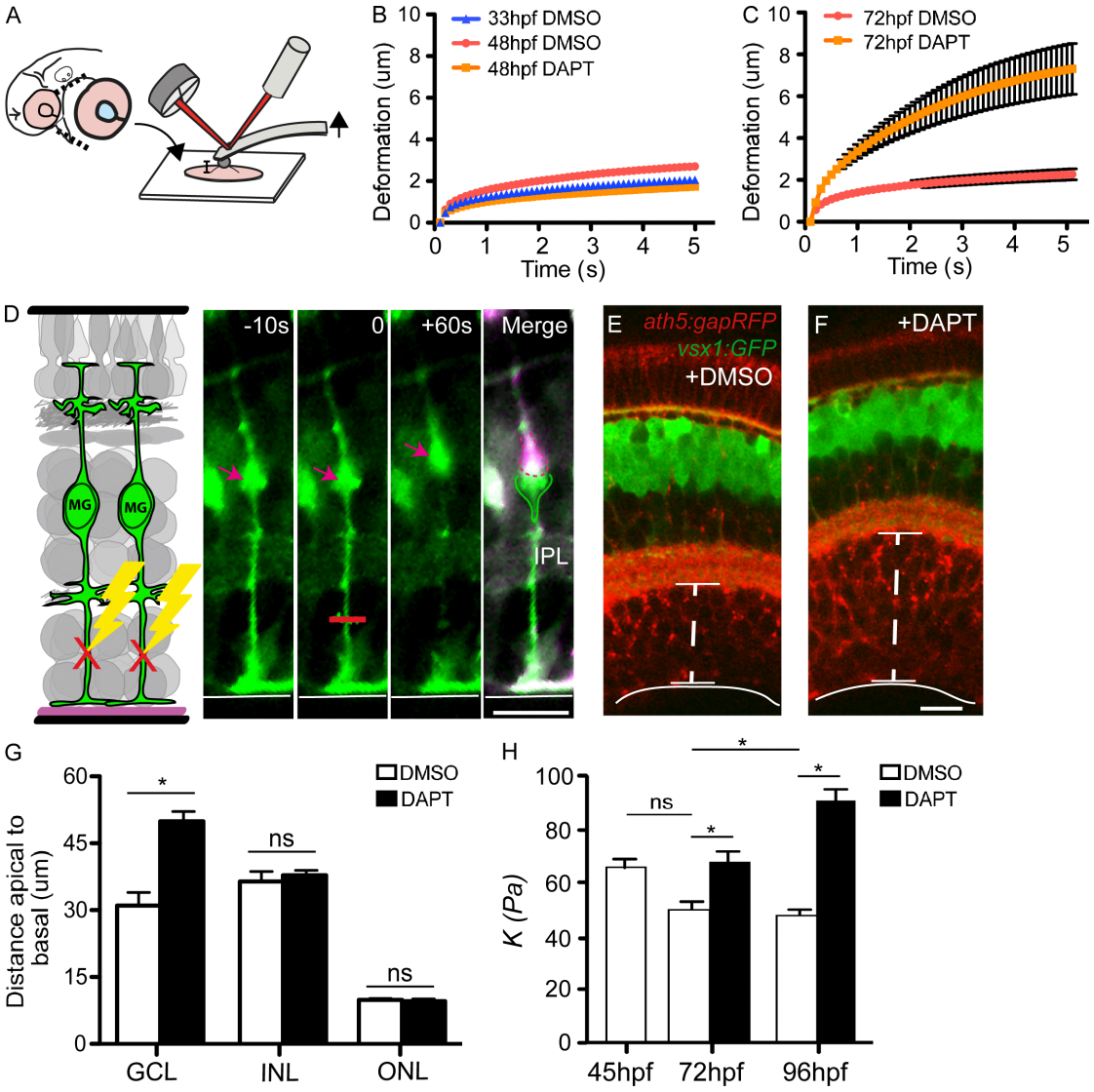

Figure 4. **MG act as springs in the retina to hold the neural retina together.** (A) To test the biophysical properties of retinas lacking MG, we used AFM to pull on the tissue. (B) Tissue deformation was not significantly different for measurements at 33 hpf or 48 hpf (mean ± SEM [error bars], *n* = 10 retinas). (C) At 72 hpf, retinas deformed significantly more when no MG were present in the tissue than controls (mean ± SEM [error bars], *n* = 10 retinas). (D) To test if MG are under strain within the retinal tissue, we applied a laser ablation technique to specifically target the apical or basal processes of *GFAP:GFP* MG in vivo. Ablating the apical process resulted in its retraction of the process and displacement of the cell body basally to the IPL. Ablation of the basal process resulted in its rapid retraction and in cell displacement apically in the INL. The merge is the overlay between each time point. Red lines delineate the regions of ablation. (E and F) Confocal images showing the expanded GCL labeled in the *ath5:gapRFP;vsx1:GFP* transgenic fish after DAPT treatment. (G) In the absence of MG, we noted a significant increase specifically in the thickness of the GCL (*n* = 20 retinas, mean + SEM [error bars], $P < 0.01$). (H) Stiffness measurements at the time of treatment (~45 hpf), 72 hpf, and 96 hpf of control and DAPT-treated retinae (*n* = 20 retinas, mean + SEM [error bars], $P < 0.01$). IPL, inner plexiform layer; ONL, outer nuclear layer. Bars, 15 µm.

resilience to the retina, while at later stage, this tensile strength rests in MG, which are the only remaining cell type to span the tissue after RPCs are gone. These results indicated that MG can act like springs (which may be put under tension) that hold the tissue together. To test if MG are normally under tension within the tissue, we used laser ablations (Fig. 4 D; Williams et al., 2010) to cut the basal processes of MG cells. After basal process ablation, the cell bodies of MG rapidly moved apically away from the inner plexiform layer (Fig. 4 D). These results are consistent with the idea that MG are normally under tension in vivo, and that when their processes are cut, this tension is released, and MG cell bodies are pulled to the side of the retina to which they are still attached.

Because MG are under tension during retinal development, they should compact the neuronal components of the retina in the apicobasal dimension. Conversely, when MG are missing, this should result in an expansion or thickening of the tissue. Indeed, in the presence of MG, the GCL was significantly thinner than in their absence (31.0 ± 2.7 µm vs. 49.9 ± 2.3 µm; $P < 0.005$, *n* = 20 retinas per condition; Fig. 4, E and G). It is important to note that there was no increase in the number of cells within the GCL in the retina (300.9 ± 7.8 with DMSO vs. 305 ± 7.96 with DAPT; $P > 0.05$; nuclei per section in the GCL at 4 d postfertilization (dpf; *n* = 10 retinas per condition), further supporting our hypothesis. However, the expansion of the tissue only occurred within the GCL, and not in the other layers.

Published September 28, 2015

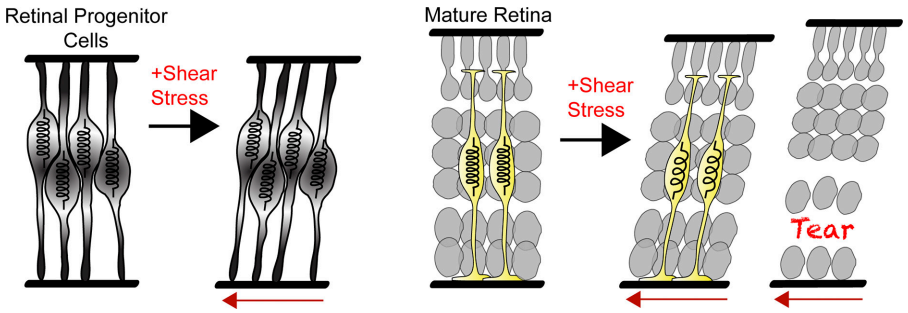

Figure 5. **Our model: Retinal progenitors behave as springs in the nascent tissue as they are radial in nature and support the tissue.** As they are depleted in the developing retina, the spring function is passed on to MG in the mature retina. However, the retina lacking MG does not have these "springs." When under mechanical stress, retinae lacking MG will deform and the tissue will rip, releasing the tension.

Importantly, in the absence of MG, it is the GCL where the retina spontaneously ripped apart. Interestingly, in culture it has been shown that providing physical support to the inner, but not to the outer, surface of the retina prevents tissue collapse and increases cell survival (Taylor et al., 2014). Thus, our data suggest that tension along MG is required for the integrity of the GCL.

Central nervous system tissue stiffens when exposed to strain (Begonia et al., 2010). Retinal tissue that is compacted by MG cells under tension should thus be stiffer, i.e., resist compressive forces more, than retinal tissue devoid of MG. To test this hypothesis, we measured the apparent elastic modulus (a measure of elastic stiffness) of the tissue by pushing on the inner retinal surface with AFM. We found, as predicted, that retinas lacking MG are significantly softer than controls (Fig. 4 H). While control retinas became stiffer with increasing age, MG-less retinas did not (Fig. 4 H). This increase in retinal stiffness with age may therefore be due to the increasing compaction of developing neural cells (Koser et al., 2015), which are squeezed together by the spring-like properties of glial cells.

In conclusion, our results suggest that MG act like taut springs that protect the neural tissue from ripping apart by holding the neural layers together (Fig. 5). This physical function is initially performed by retinal neuroepithelial cells in the nascent tissue and then taken over by the MG once they are born and the neuroepithelial cells have differentiated into neurons. In the absence of the MG in the mature tissue, there are no cells spanning the tissue present, and it becomes susceptible to shear and tensile forces, eventually leading to ripping. Thus, the presence of MG likely makes the retina more resistant to deformation. This is a critical function, as the vertebrate retina is constantly exposed to dynamic shear forces and tension (Lu et al., 2006; Franze et al., 2011), especially along its inner surface (Marmor, 1993). How MG provide tensile strength is yet unclear, but both RPCs at early stages and MG at later stages abundantly express the intermediate filament Vimentin (Shaw and Weber, 1984; Jones and Schechter, 1987). Vimentin networks stiffen under load (Janmey et al., 1991). The expression of intermediate filaments may therefore be an adaptation of glial cells to optimize their mechanical function. Our results may help explain the similar ripping of retinae in mice deficient for GFAP and Vimentin induced by indirect mechanical stress (Lundkvist et al., 2004). The intermediate filaments in MG cells may thus provide structural support to the retina, much as collagen fibers do in the skin (Fratzl, 2008). It would therefore be interesting to examine whether glial cells elsewhere in the brain also provide mechanical resilience to neural structures. Our study demonstrates that at least one type of glial cell, the MG in the retina, do indeed act like "nerve putty" and physically support neurons in vivo.

Materials and methods

Zebrafish maintenance

Zebrafish were maintained and bred at 26.5°C. All animal work was approved by Local Ethical Review Committee at the University of Cambridge, and performed according to the protocols of project license PPL 80/2198 and to the institutional guidelines (IACUC) of the University of Washington.

Embryo manipulations

Embryos used for whole-mount imaging were treated with 0.003% phenylthiourea (Sigma-Aldrich) from 10 hpf to prevent pigmentation. Embryos used for sections were fixed with 4% paraformaldehyde and cryoprotected in 30% sucrose in 1× PBS overnight before cryosectioning. Morpholino injections for Su(H) (sequence: 5′-CGCCATCTTCACC AACTCTCTCTAA-3′; Sieger et al., 2003) and her4.3 (sequence: 5′-TTGATCCAGTGATTGTAGGAGTCAT-3′; Pasini et al., 2004) were performed using a previously described morpholino oligonucleotide at similar concentrations. The control morpholino was injected at a similar concentration (sequence: 5′-CCTCTTACCTCAGTTACAATTTATA-3′).

For blastomere transplantations, high- to oblong-stage embryos were dechorionated by pronase digestion (Sigma-Aldrich) and placed in agarose molds, and between 5 and 30 blastomeres were transferred between embryos using a glass capillary connected to a 2 ml syringe.

Zebrafish embryos were continuously treated with DAPT (25–50 µM) or Compound E (10 µM) in 0.5% DMSO in E3 embryo media from ∼45 hpf up to 5 dpf. Control embryos were treated with 0.5% DMSO in E3 media. Media was changed daily.

Transgenic lines and constructs

Transgenic lines Tg(*TP1bglob:VenusPEST*)^{S940} (Ninov et al., 2012), Tg(*her4.1:mCherry,Cre-ERT2*) (Kroehne et al., 2011), and Tg(*her4.3:EGFP*) (Yeo et al., 2007) were used to report on Notch signaling in the retina. Tg(*gfap:GFP*)^{mi6} (Bernardos and Raymond, 2006) and Tg(*GFAP:dTomato*) (a gift from S. Higashijima, National Institutes of Natural Sciences, Okazaki, Japan; Satou et al., 2012) were used to label glial cells in the retina. Tg(*atoh7:gap43-mRFP1*)^{cu2} (Zolessi et al., 2006), Tg(*vsx1:GFP*)^{nns5} (Kimura et al., 2008), and Tg(*crx:CFP; ptf1a-Gal4:UAS-YFP; atoh7:gap43-mRFP1*^{cu2}) (Almeida et al., 2014) were used to label retinal neurons. Tg(*betaActin:H2B-GFP*) (He et al., 2012) was used to label all nuclei in the retina. These transgenes are abbreviated hereafter as *TP1:Venus*, *GFAP:dTomato*, *ath5:gapRFP*, *vsx1:GFP*, *GFAP:GFP*, *SoFa*, *H2B:GFP*, *Her4:Cherry*, and her4:GFP.

Confocal imaging and immunostaining

Confocal imaging of live embryos was performed at ∼28°C and fixed embryos at ∼22°C, as described previously (Das et al., 2003). Laser scanning confocal imaging was performed using a microscope (FV1000; Olympus) with a 60× silicon oil immersion objective lens (1.3 NA) using the FV10-ASW software (Version 4.2; Olympus), or

Published September 28, 2015

cryosections with an SP2 microscope (Leica) with a 63× (1.2 NA) water immersion objective lens using the LCS Leica Confocal Software (Leica). Image analysis was performed using ImageJ or Volocity Software (PerkinElmer).

Immunostaining was performed using Alexa Fluor–conjugated secondary antibodies (Invitrogen) and the following primary antibodies: mouse anti–glutamine synthase (GS; 1:50, mab302; Millipore), rabbit polyclonal anti-Cralbp (antigen bovine CRALBP [UW55]; 1:1,000; a gift from J. Saari, University of Washington, Seattle, WA), mouse anti-GFAP (1:100 zrf1; ZIRC), rabbit anti-carbonic anhydrase (1:200, ab108367; Abcam), rabbit anti-Harmonin (1:200, 2090-00-02; Sdix), rabbit anti-BLBP (1:200, ab32423; Abcam), rabbit anti-Sox2 (1:150, ab5603; Millipore), mouse anti-Vimentin (1:100, 40E-C; Developmental Studies Hybridoma Bank), rabbit anti-BLBP (1:100, ab32423; Abcam), mouse anti-Rs1 (1:200, ab167579; Abcam), mouse anti-zpr1(1:100; ZIRC), and rabbit anti-rhodopsin (1:100, ab3424; Abcam). Cryosections were taken at 12 µm thickness using a Jung Frigocut cryostat (Leica).

TUNEL staining and nuclei counting

Slides were stained with an in situ cell death detection kit, TMR Red from Roche for 1.5 h at 37°C. The slides were washed in 1× PBS for 5 min and mounted with Vectashield Hard Set medium with DAPI (#H-1500). Only sections containing the lens, corresponding to the central retina, were imaged and quantified. To count the number of cells in the GCL, DAPI+ nuclei were counted per section (12 µm thick) in DMSO control and DAPT experimental conditions at 4 dpf.

Transmission electron microscopy

Zebrafish embryos and larvae were fixed at 6 d after fertilization with 4% glutaraldehyde in 0.1 M sodium cacodylate buffer, pH 7.4, for several hours. After washing in buffer, they were postfixed in 1% OsO_4 in cacodylate buffer and stained en bloc with 1% uranyl acetate. After immersion in a graded ethanol series, the animals were embedded in Araldite, sectioned, and stained with 1% lead citrate before imaging.

AFM

Embryos (33–96 hpf) were anesthetized with MS-222 (tricaine, 0.02%), the lens was removed, and the retina was microdissected in 1× Danieau's solution (58 mM NaCl, 0.7 mM KCl, 0.4 mM $MgSO_4$, 0.6 mM Ca $(NO_3)_2$, and 5 mM Hepes, pH 7.6), washed in 1× Danieau's solution for 5 min, and mounted with the nerve fiber layer facing up on glass slides with adhesive Cell-Tak (BD). Polystyrene beads (diameter = 37 µm) were glued to tipless silicon cantilevers (ARROW-TL1-50, spring constant ∼0.01 N/m; Nano World), coated with Cell-Tak and mounted on the AFM (CellHesion 200; JPK Instruments AG). Cantilevers were calibrated with the thermal noise method, which is built into the AFM software. For tensile measurements, cantilevers were brought in contact with the retinae (with F = 2nN until the bead firmly adhered to the tissue (∼30 s). Subsequently, the cantilever was retracted with F = −5nN, thus pulling on the retina for 5 s, and tissue deformation was measured. Retraction curves were smooth, indicating that there were no sudden rips (i.e., tearing) of the tissue during the experiment. Using the described AFM parameters, control and DAPT-treated retinae had triplicate measurements taken per sample (n = 20). Measurements of control and treated retinae were alternated to avoid bias.

Stiffness measurements were taken using the same AFM parameters and tissue preparations with the exception that beaded cantilevers (not treated with CellTak) were used to indent the samples and determine their resistance to the applied force (i.e., their apparent elastic modulus $K = E/(1 - \nu^2)$, where E is the Young's modulus and ν is the Poisson's ratio). Control and treated retinae were prepared one at a time and measured alternatively to avoid bias. For each retina, 20 measurements at random positions were recorded. Data were analyzed using custom software built in MatLab fitting the Hertz model to the data (Christ et al., 2010): $F = \frac{4}{3}K\sqrt{R}\,\delta^{3/2}$, where R is the radius of the indenter and δ is the indentation depth.

MG process ablations

Multiphoton image stacks were acquired on a two-photon excitation fluorescence scanning microscope (TriM Scope II; LaVision BioTec). The system used a laser system (InSight DeepSee; Spectra Physics) as the light source tuned to 927 nm for optimal excitation of GFP. To perform successful targeted ablation, we used ∼300 mW average power femtosecond pulses scanned over a 100 µm × 100 µm area (208 × 208 pixels) with an 11-ms dwell time. Imaging of 5 µm deep volume allowed planes above and below the ablated region to be imaged. This verified the localized nature of the ablation and the effects to be monitored over a larger volume. Data stacks were acquired at a rate of 0.5 Hz, with 50 time points taken before and 300 taken after the point of treatment.

Data analysis and statistics

As all data were normally distributed (as determined by the Kolmogorov-Smirnov test), differences were tested using the two-tailed Student's t test, and an ANOVA test in the case of three or more groups. Newman-Keuls and Dunn's tests were used as multiple-comparison post hoc tests. All values given in the text are mean values ± SEM.

Online supplemental material

Fig. S1 shows that additional MG markers are lost in DAPT-treated retinas. Fig. S2 shows that the retina before MG are generated and the severity of the retinoschisis phenotype without MG. Fig. S3 shows additional cellular defects in the retina lacking MG. Video 1 is a time lapse of Notch activity within clones in the embryonic zebrafish retina. Videos 2 and 3 are confocal stacks through the retina in control and DAPT-treated retinas at 96 hpf. Online supplemental material is available at http://www.jcb.org/cgi/content/full/jcb.201503115/DC1. Additional data are available in the JCB DataViewer at http://dx.doi.org/10.1083/jcb.201503115.dv.

Acknowledgments

We acknowledge R.O. Wong and E. Parker for electron microscopy assistance, K. O'Holleran and the Cambridge Advanced Imaging Centre (CAIC) for two-photon microscopy assistance, and A. Almeida for image analysis and careful reading of the manuscript.

This work was funded by a Herchel Smith Postdoctoral Fellowship to R.B. MacDonald, the Wellcome Trust program in Developmental Biology to O. Randlett and J. Oswald, National Institutes of Health grants EY14358 (to R.O. Wong, University of Washington) and EY01730 (Vision Core), an Medical Research Council Career Development Award, a Human Frontier Science Program Young Investigator Grant to K. Franze, and a Wellcome Trust Investigator Award to W.A. Harris.

The authors declare no competing financial interests.

Author contributions: R.B. MacDonald, K. Franze, and W.A. Harris designed the experiments and wrote the manuscript. R.B. MacDonald, O. Randlett, J. Oswald, and T. Yoshimatsu performed the experiments and data analysis. O. Randlett and T. Yoshimatsu revised the manuscript.

Submitted: 25 March 2015
Accepted: 13 August 2015

Published September 28, 2015

References

Allen, N.J., and B.A. Barres. 2009. Neuroscience: Glia - more than just brain glue. *Nature.* 457:675–677. http://dx.doi.org/10.1038/457675a

Almeida, A.D., H. Boije, R.W. Chow, J. He, J. Tham, S.C. Suzuki, and W.A. Harris. 2014. Spectrum of Fates: a new approach to the study of the developing zebrafish retina. *Development.* 141:1971–1980. http://dx.doi.org/10.1242/dev.104760

Aulehla, A., W. Wiegraebe, V. Baubet, M.B. Wahl, C. Deng, M. Taketo, M. Lewandoski, and O. Pourquié. 2008. A β-catenin gradient links the clock and wavefront systems in mouse embryo segmentation. *Nat. Cell Biol.* 10:186–193. http://dx.doi.org/10.1038/ncb1679

Begonia, M.T., R. Prabhu, J. Liao, M.F. Horstemeyer, and L.N. Williams. 2010. The influence of strain rate dependency on the structure-property relations of porcine brain. *Ann. Biomed. Eng.* 38:3043–3057. http://dx.doi.org/10.1007/s10439-010-0072-9

Bernardos, R.L., and P.A. Raymond. 2006. GFAP transgenic zebrafish. *Gene Expr. Patterns.* 6:1007–1013. http://dx.doi.org/10.1016/j.modgep.2006.04.006

Bernardos, R.L., S.I. Lentz, M.S. Wolfe, and P.A. Raymond. 2005. Notch–Delta signaling is required for spatial patterning and Müller glia differentiation in the zebrafish retina. *Dev. Biol.* 278:381–395. http://dx.doi.org/10.1016/j.ydbio.2004.11.018

Bringmann, A., T. Pannicke, J. Grosche, M. Francke, P. Wiedemann, S.N. Skatchkov, N.N. Osborne, and A. Reichenbach. 2006. Müller cells in the healthy and diseased retina. *Prog. Retin. Eye Res.* 25:397–424. http://dx.doi.org/10.1016/j.preteyeres.2006.05.003

Byrne, L.C., F. Khalid, T. Lee, E.A. Zin, K.P. Greenberg, M. Visel, D.V. Schaffer, and J.G. Flannery. 2013. AAV-mediated, optogenetic ablation of Müller glia leads to structural and functional changes in the mouse retina. *PLoS ONE.* 8:e76075. http://dx.doi.org/10.1371/journal.pone.0076075

Byrne, L.C., B.E. Oztürk, T. Lee, C. Fortuny, M. Visel, D. Dalkara, D.V. Schaffer, and J.G. Flannery. 2014. Retinoschisin gene therapy in photoreceptors, Müller glia or all retinal cells in the Rs1h-/- mouse. *Gene Ther.* 21:585–592. http://dx.doi.org/10.1038/gt.2014.31

Cajal, S.R. 1972. The Structure of the Retina. S.A. Thorpe, and M. Glickstein, editors. Charles Thomas, Illinois. 196 pp.

Christ, A.F., K. Franze, H. Gautier, P. Moshayedi, J. Fawcett, R.J. Franklin, R.T. Karadottir, and J. Guck. 2010. Mechanical difference between white and gray matter in the rat cerebellum measured by scanning force microscopy. *J. Biomech.* 43:2986–2992. http://dx.doi.org/10.1016/j.jbiomech.2010.07.002

Das, T., B. Payer, M. Cayouette, and W.A. Harris. 2003. In vivo time-lapse imaging of cell divisions during neurogenesis in the developing zebrafish retina. *Neuron.* 37:597–609. http://dx.doi.org/10.1016/S0896-6273(03)00066-7

Dorsky, R.I., D.H. Rapaport, and W.A. Harris. 1995. Xotch inhibits cell differentiation in the *Xenopus* retina. *Neuron.* 14:487–496. http://dx.doi.org/10.1016/0896-6273(95)90305-4

Easter, S.S. Jr., and G.N. Nicola. 1996. The development of vision in the zebrafish (*Danio rerio*). *Dev. Biol.* 180:646–663. http://dx.doi.org/10.1006/dbio.1996.0335

Franze, K. 2011. Atomic force microscopy and its contribution to understanding the development of the nervous system. *Curr. Opin. Genet. Dev.* 21:530–537. http://dx.doi.org/10.1016/j.gde.2011.07.001

Franze, K., M. Francke, K. Guenter, A.F. Christ, N. Koerber, A. Reichenbach, and J. Guck. 2011. Spatial mapping of the mechanical properties of the living retina using scanning force microscopy. *Soft Matter.* 7:3147–3154. http://dx.doi.org/10.1039/c0sm01017k

Franze, K., P.A. Janmey, and J. Guck. 2013. Mechanics in neuronal development and repair. *Annu. Rev. Biomed. Eng.* 15:227–251. http://dx.doi.org/10.1146/annurev-bioeng-071811-150045

Fratzl, P., editor. 2008. Collagen: Structure and Mechanics. Springer, New York. 506 pp. http://dx.doi.org/10.1007/978-0-387-73906-9

Furukawa, T., S. Mukherjee, Z.Z. Bao, E.M. Morrow, and C.L. Cepko. 2000. rax, Hes1, and notch1 promote the formation of Müller glia by postnatal retinal progenitor cells. *Neuron.* 26:383–394. http://dx.doi.org/10.1016/S0896-6273(00)81171-X

Green, E.S., J.L. Stubbs, and E.M. Levine. 2003. Genetic rescue of cell number in a mouse model of microphthalmia: interactions between Chx10 and G1-phase cell cycle regulators. *Development.* 130:539–552. http://dx.doi.org/10.1242/dev.00275

He, J., G. Zhang, A.D. Almeida, M. Cayouette, B.D. Simons, and W.A. Harris. 2012. How variable clones build an invariant retina. *Neuron.* 75:786–798. http://dx.doi.org/10.1016/j.neuron.2012.06.033

Hu, M., and S.S. Easter. 1999. Retinal neurogenesis: the formation of the initial central patch of postmitotic cells. *Dev. Biol.* 207:309–321. http://dx.doi.org/10.1006/dbio.1998.9031

Janmey, P.A., U. Euteneuer, P. Traub, and M. Schliwa. 1991. Viscoelastic properties of vimentin compared with other filamentous biopolymer networks. *J. Cell Biol.* 113:155–160. http://dx.doi.org/10.1083/jcb.113.1.155

Jones, P.S., and N. Schechter. 1987. Distribution of specific intermediate-filament proteins in the goldfish retina. *J. Comp. Neurol.* 266:112–121. http://dx.doi.org/10.1002/cne.902660109

Kay, J.N., K.C. Finger-Baier, T. Roeser, W. Staub, and H. Baier. 2001. Retinal ganglion cell genesis requires *lakritz*, a zebrafish atonal homolog. *Neuron.* 30:725–736. http://dx.doi.org/10.1016/S0896-6273(01)00312-9

Kettenmann, H., and B.R. Ransom. 2013. Neuroglia. Third edition. Oxford University Press, New York, USA. 864 pp.

Kimura, Y., C. Satou, and S. Higashijima. 2008. V2a and V2b neurons are generated by the final divisions of pair-producing progenitors in the zebrafish spinal cord. *Development.* 135:3001–3005. http://dx.doi.org/10.1242/dev.024802

Koser, D.E., E. Moeendarbary, J. Hanne, S. Kuerten, and K. Franze. 2015. CNS cell distribution and axon orientation determine local spinal cord mechanical properties. *Biophys. J.* 108:2137–2147. http://dx.doi.org/10.1016/j.bpj.2015.03.039

Kroehne, V., D. Freudenreich, S. Hans, J. Kaslin, and M. Brand. 2011. Regeneration of the adult zebrafish brain from neurogenic radial glia-type progenitors. *Development.* 138:4831–4841. http://dx.doi.org/10.1242/dev.072587

Lindqvist, N., Q. Liu, J. Zajadacz, K. Franze, and A. Reichenbach. 2010. Retinal glial (Müller) cells: sensing and responding to tissue stretch. *Invest. Ophthalmol. Vis. Sci.* 51:1683–1690. http://dx.doi.org/10.1167/iovs.09-4159

Lu, Y.B., K. Franze, G. Seifert, C. Steinhäuser, F. Kirchhoff, H. Wolburg, J. Guck, P. Janmey, E.Q. Wei, J. Käs, and A. Reichenbach. 2006. Viscoelastic properties of individual glial cells and neurons in the CNS. *Proc. Natl. Acad. Sci. USA.* 103:17759–17764. http://dx.doi.org/10.1073/pnas.0606150103

Lundkvist, A., A. Reichenbach, C. Betsholtz, P. Carmeliet, H. Wolburg, and M. Pekny. 2004. Under stress, the absence of intermediate filaments from Müller cells in the retina has structural and functional consequences. *J. Cell Sci.* 117:3481–3488. http://dx.doi.org/10.1242/jcs.01221

Marmor, M.F. 1993. Mechanisms of retinal adhesion. *Prog. Retinal Res.* 12:179–204. http://dx.doi.org/10.1016/0278-4327(93)90009-I

Molday, R.S., U. Kellner, and B.H. Weber. 2012. X-linked juvenile retinoschisis: clinical diagnosis, genetic analysis, and molecular mechanisms. *Prog. Retin. Eye Res.* 31:195–212. http://dx.doi.org/10.1016/j.preteyeres.2011.12.002

Ninov, N., M. Borius, and D.Y. Stainier. 2012. Different levels of Notch signaling regulate quiescence, renewal and differentiation in pancreatic endocrine progenitors. *Development.* 139:1557–1567. http://dx.doi.org/10.1242/dev.076000

Parsons, M.J., H. Pisharath, S. Yusuff, J.C. Moore, A.F. Siekmann, N. Lawson, and S.D. Leach. 2009. Notch-responsive cells initiate the secondary transition in larval zebrafish pancreas. *Mech. Dev.* 126:898–912. http://dx.doi.org/10.1016/j.mod.2009.07.002

Pasini, A., Y.J. Jiang, and D.G. Wilkinson. 2004. Two zebrafish Notch-dependent *hairy/Enhancer-of-split-related* genes, *her6* and *her4*, are required to maintain the coordination of cyclic gene expression in the presomitic mesoderm. *Development.* 131:1529–1541. http://dx.doi.org/10.1242/dev.01031

Randlett, O., R.B. MacDonald, T. Yoshimatsu, A.D. Almeida, S.C. Suzuki, R.O. Wong, and W.A. Harris. 2013. Cellular requirements for building a retinal neuropil. *Cell Reports.* 3:282–290. http://dx.doi.org/10.1016/j.celrep.2013.01.020

Rapaport, D.H., L.L. Wong, E.D. Wood, D. Yasumura, and M.M. LaVail. 2004. Timing and topography of cell genesis in the rat retina. *J. Comp. Neurol.* 474:304–324. http://dx.doi.org/10.1002/cne.20134

Reichenbach, A., and A. Bringmann. 2013. New functions of Müller cells. *Glia.* 61:651–678. http://dx.doi.org/10.1002/glia.22477

Reid, S.N., and D.B. Farber. 2005. Glial transcytosis of a photoreceptor-secreted signaling protein, retinoschisin. *Glia.* 49:397–406. http://dx.doi.org/10.1002/glia.20131

Samuels, B., and A. Fuchs. 1952. Clinical Pathology of the Eye: A Practical Treatise of Histopathology. Hoeber, New York. 420 pp.

Satou, C., Y. Kimura, and S. Higashijima. 2012. Generation of multiple classes of V0 neurons in zebrafish spinal cord: progenitor heterogeneity and temporal control of neuronal diversity. *J. Neurosci.* 32:1771–1783. http://dx.doi.org/10.1523/JNEUROSCI.5500-11.2012

Sauer, C.G., A. Gehrig, R. Warneke-Wittstock, A. Marquardt, C.C. Ewing, A. Gibson, B. Lorenz, B. Jurklies, and B.H. Weber. 1997. Positional cloning of the gene associated with X-linked juvenile retinoschisis. *Nat. Genet.* 17:164–170. http://dx.doi.org/10.1038/ng1097-164

Shaw, G., and K. Weber. 1984. The intermediate filament complement of the retina: a comparison between different mammalian species. *Eur. J. Cell Biol.* 33:95–104.

Shen, W., M. Fruttiger, L. Zhu, S.H. Chung, N.L. Barnett, J.K. Kirk, S. Lee, N.J. Coorey, M. Killingsworth, L.S. Sherman, and M.C. Gillies. 2012. Conditional Müllercell ablation causes independent neuronal and vascular pathologies in a novel transgenic model. *J. Neurosci.* 32:15715–15727. http://dx.doi.org/10.1523/JNEUROSCI.2841-12.2012

Shreiber, D.I., H. Hao, and R.A. Elias. 2009. Probing the influence of myelin and glia on the tensile properties of the spinal cord. *Biomech. Model. Mechanobiol.* 8:311–321. http://dx.doi.org/10.1007/s10237-008-0137-y

Sieger, D., D. Tautz, and M. Gajewski. 2003. The role of Suppressor of Hairless in Notch mediated signalling during zebrafish somitogenesis. *Mech. Dev.* 120:1083–1094. http://dx.doi.org/10.1016/S0925-4773(03)00154-0

Straatsma, B.R., and R.Y. Foss. 1973. Typical and reticular degenerative retinoschisis. *Am. J. Ophthalmol.* 75:551–575. http://dx.doi.org/10.1016/0002-9394(73)90809-X

Swift, J., I.L. Ivanovska, A. Buxboim, T. Harada, P.C. Dingal, J. Pinter, J.D. Pajerowski, K.R. Spinler, J.W. Shin, M. Tewari, et al. 2013. Nuclear lamin-A scales with tissue stiffness and enhances matrix-directed differentiation. *Science.* 341:1240104. http://dx.doi.org/10.1126/science.1240104

Taylor, L., K. Arnér, I.H. Taylor, and F. Ghosh. 2014. Feet on the ground: Physical support of the inner retina is a strong determinant for cell survival and structural preservation in vitro. *Invest. Ophthalmol. Vis. Sci.* 55:2200–2213. http://dx.doi.org/10.1167/iovs.13-13535

Tomita, K., K. Moriyoshi, S. Nakanishi, F. Guillemot, and R. Kageyama. 2000. Mammalian achaete-scute and atonal homologs regulate neuronal versus glial fate determination in the central nervous system. *EMBO J.* 19:5460–5472. http://dx.doi.org/10.1093/emboj/19.20.5460

Virchow, R. 1856. Gesammelte Abhandlungen zur Wissenschaftlichen Medicin. von Meidinger Sohn, Frankfurt, Germany. 1024 pp.

Williams, P.R., S.C. Suzuki, T. Yoshimatsu, O.T. Lawrence, S.J. Waldron, M.J. Parsons, M.L. Nonet, and R.O. Wong. 2010. In vivo development of outer retinal synapses in the absence of glial contact. *J. Neurosci.* 30:11951–11961. http://dx.doi.org/10.1523/JNEUROSCI.3391-10.2010

Yeo, S.Y., M. Kim, H.S. Kim, T.L. Huh, and A.B. Chitnis. 2007. Fluorescent protein expression driven by her4 regulatory elements reveals the spatiotemporal pattern of Notch signaling in the nervous system of zebrafish embryos. *Dev. Biol.* 301:555–567. http://dx.doi.org/10.1016/j.ydbio.2006.10.020

Zolessi, F.R., L. Poggi, C.J. Wilkinson, C.B. Chien, and W.A. Harris. 2006. Polarization and orientation of retinal ganglion cells in vivo. *Neural Dev.* 1:2. http://dx.doi.org/10.1186/1749-8104-1-2

MacDonald et al., http://www.jcb.org/cgi/content/full/jcb.201503115/DC1

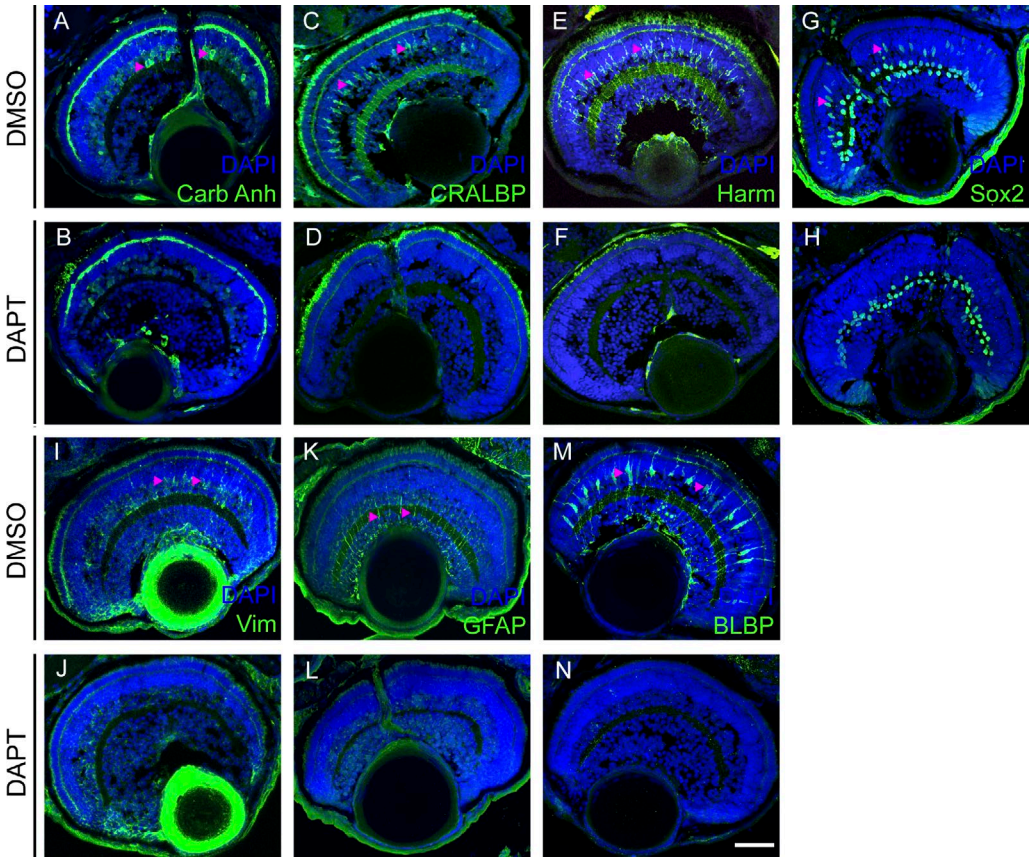

Figure S1. **Blocking Notch with DAPT results in retinas lacking expression of several MG immunohistochemical markers at 96 hpf.** Control retinas are treated with DMSO. DAPT-treated retinas show no expression of MG-specific markers. Shown are carbonic anhydrase (A and B), Cralbp (C and D), Harmonin (E and F), Sox2 (G and H), Vimentin (I and J), GFAP (K and L), and BLBP (M and N). Arrowheads point to MG. Bar, 50 µm.

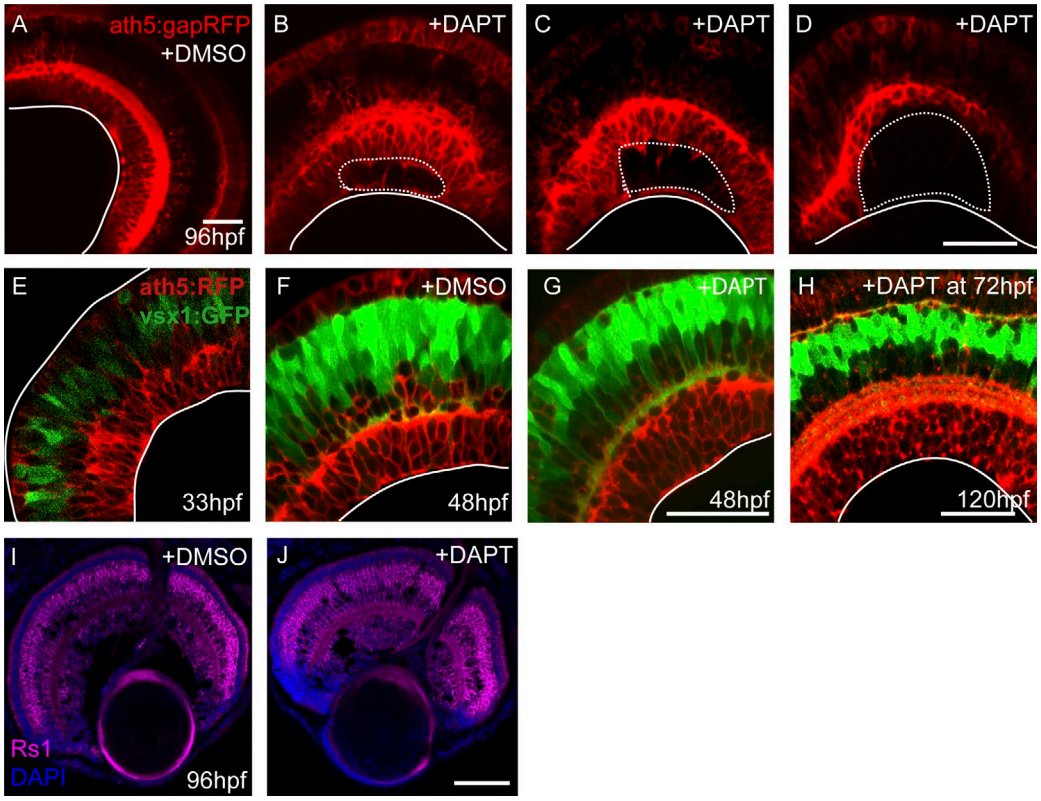

Figure S2. **The extent of ripping in the GCL varies in the absence of MG.** Single z-sections of unfixed transgenic retinas are shown. (A–D) *ath5:gapRFP* strongly labels the GCL. The retinoschisis phenotype varies in severity from retina to retina. The basal surface of the retina is marked with a solid line. The rip is marked with a broken line. (E–H) In the *vsx1:GFP;ath5:gapRFP* transgenic embryos, most retinal neurons are labeled. There is no evidence of ripping within the nascent retina at 33 hpf (E) and 48 hpf (F), when radial progenitors remain and MG would normally not be present. (G) Just after DAPT is added to the media, there are no rips in the retina. (H) Treatment of the embryo with DAPT after 72 hpf, allowing MG to be specified in the central retina, does not result in rips 48 h later. (I) her4:GFP is expressed specifically in the bipolar cells (arrow) and MG (arrowhead) in the retina. (J) Knockdown of her4 expression reduces the number of MG and results in the retinoschisis phenotype in the GCL. (K and L) Cryosection of the retina showing that Retinoschisin1 expression is not altered with DAPT treatment at 96 hpf. Bars: (A) 30 µm; (B–D) 25 µm; (E–H) 30 µm; (J) 50 µm.

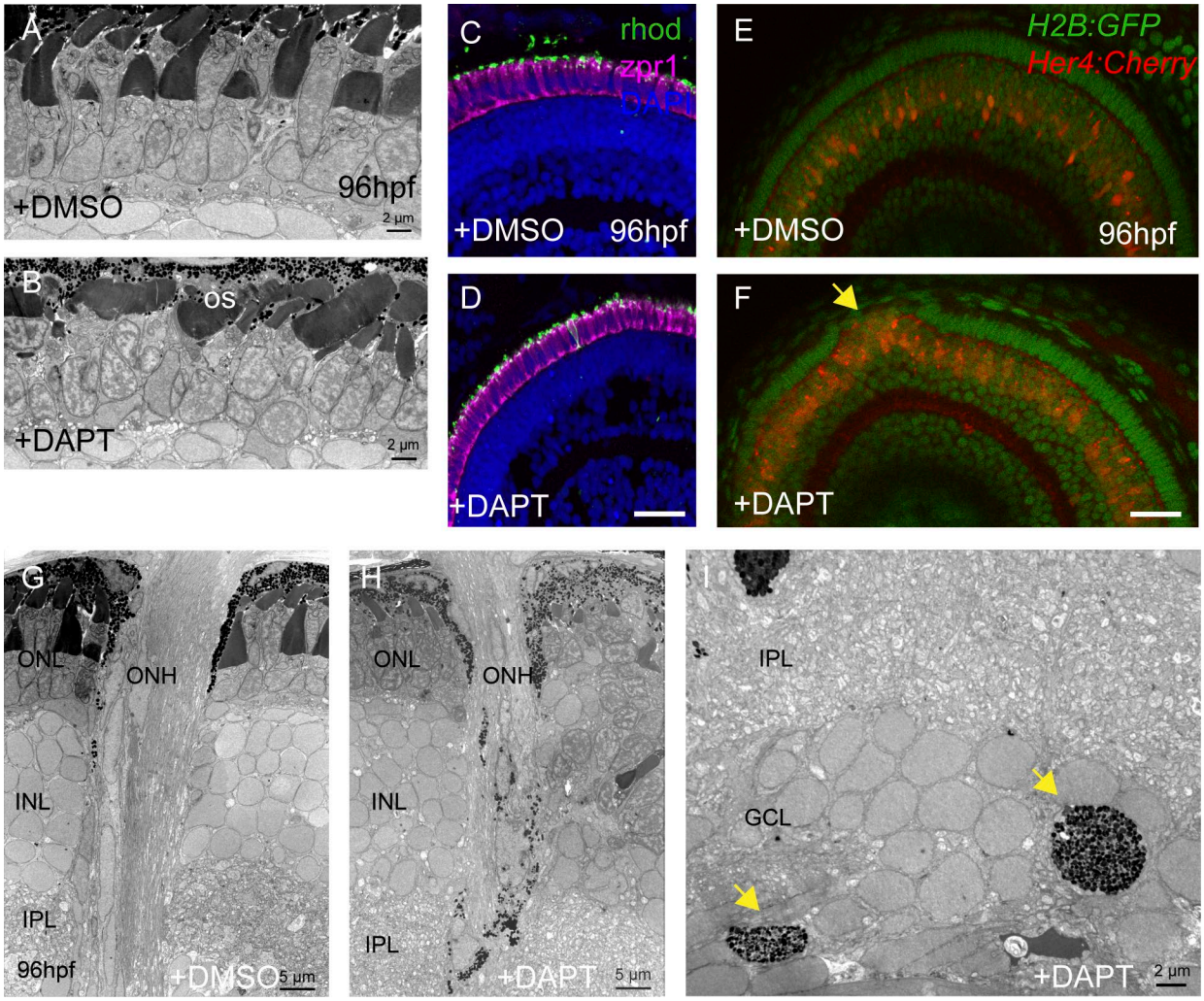

Figure S3. **Defects in the retina lacking MG (related to Fig. 2).** Electron micrographs of the retina lacking MG. (A and B) Photoreceptor cell bodies and their outer segments appear disorganized in DAPT-treated retinas. (C and D) Despite a disorganized outer nuclear layer (ONL), both rods and cones are present in the DAPT-treated retinas, as labeled by rhodopsin and zpr1, respectively. (E and F) However, the photoreceptor layer is occasionally disrupted (n = 1/20 fish; arrow), as shown by the *H2B:GFP* transgene, where all nuclei are labeled (green). (G–I) Electron micrographs show pigmentation extending along the optic nerve head into the retina with DAPT treatment. Pigment granules can also be found in the GCL upon DAPT treatment (I, arrows). ONH, optic nerve head; IPL, inner plexiform layer. Bars in C–F, 30 µm.

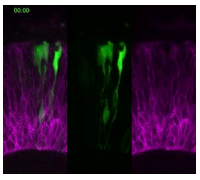

Video 1. **In vivo time lapse of Notch activity within clones in the embryonic retina.** Time-lapse confocal imaging of mosaic retinas with *TP1:Venus* (green)-labeled clones within host retinas where many retinal neurons are labeled by *ath5:gapRFP* (magenta). Images are of maximum-intensity projections of five confocal slices from time-lapse confocal microscopy using a laser-scanning confocal microscope (FV1000; Olympus). Time is shown in hours:minutes. Imaging begins at ~38 hpf and frames were taken every 15 min for ~24 h. n = 6 clones observed.

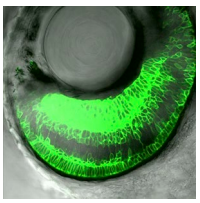

Video 2. **There is no retinoschisis in the retina under control conditions.** Single z stack captured in vivo from a DMSO control *ath5:GAP-RFP* (green) zebrafish retina at 96 hpf using a laser-scanning confocal microscope (FV1000; Olympus). The step size is 2 µm and the video is displayed at 10 frames per second.

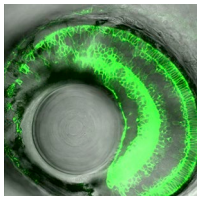

Video 3. **There is a significant retinoschisis phenotype in the retina in the absence of MG.** Single z stack captured in vivo from a DAPT control *ath5:GAP-RFP* (green) zebrafish retina at 96 hpf using a laser-scanning confocal microscope (FV1000; Olympus). The step size is 2 µm and the video is displayed at 10 frames per second.